RSC Advances

PAPER

Cite this: *RSC Adv.*, 2024, **14**, 3691

The role of non-covalent interactions in 4-hydroxybenzylamine macrocyclisation: computational and synthetic evidence†

Andrés Gonzalez-Oñate, Jorge Alí-Torres and Rodolfo Quevedo *

Received 13th December 2023
Accepted 16th January 2024

DOI: 10.1039/d3ra08508b

rsc.li/rsc-advances

4-hydroxybenzylamine's intermolecular interactions and their possible influence on the course of 4-hydroxybenzylamine's reaction with formaldehyde are analysed in this article. Computational calculations established that 4-hydroxybenzylamine forms dimers in solution by O–H···N hydrogen bonds; such dimers are stabilised by π-stacking interactions. These cyclic dimers' formation led to obtaining a 12-atom azacyclophane through 4-hydroxybenzylamine's reaction with formaldehyde.

Introduction

Cyclophanes are macrocyclic compounds containing two or more aromatic rings which are bound to their *meta* or *para* positions by short spacers.[1] Such compounds are of interest due to their ability to retain ions or molecules within their cavity through non-covalent interactions.[2–6] Azacyclophanes are cyclophanes which contain nitrogen atoms in their spacers. These compounds combine cyclophane characteristics with nitrogen's acid–base properties; such combination makes them good candidates for host-guest interaction-related studies.[2–7] Their molecular topology, cavity size and solubility depend on the spacer length and the functional groups in the aromatic rings or spacers.[4,8–10]

14-Atom azacyclophane synthesis *via* 4-hydroxyphenylethylamine reaction with formaldehyde has been reported in the pertinent literature; these azacyclophanes' structure is formed by two 3,4-dihydro-2*H*-1,3-benzoxazine units joined by ethylene bridges.[11,12] It has been proposed that macrocyclisation depends on template formation (cyclic dimers) by hydrogen bonds (O–H···N) between phenolic hydroxyls and amino groups having two 4-hydroxyphenylethylamine molecules; this strategy has been called hydrogen bond-assisted macrocyclic synthesis (Scheme 1). Macrocyclisation does not occur when template formation is not promoted by electronic or steric factors; only linear oligomer mixtures are obtained.[13–16]

The hydrogen bond-assisted macrocyclic synthesis strategy has only been used for obtaining 14-atom azacyclophanes to date. This article thus describes analysing hydrogen bond-derived template formation using computational calculations; the 4-hydroxybenzylamine (4-(aminomethyl)phenol) **1** and formaldehyde condensation product was isolated and characterised using various solvents for establishing whether 12-atom azacyclophanes could be obtained by 4-hydroxybenzylamine **1** reaction with formaldehyde.

Experimental

General

Commercially available solvents and reagents were used (Alfa Aesar, Panreac). Thin layer chromatography (TLC) was used for monitoring the reactions on silica gel-coated glass plates (Merck Kieselgel 60) until completion; the TLC plates were visualised by staining with iodine vapor. A Mel-Temp digital melting point electrothermal 9100 apparatus was used for determining the melting points, using open capillaries; the reported results have not been corrected. NMR spectra were recorded on a Bruker Avance. Chemical shifts (δ) were reported in parts per million (ppm, from the residual solvent peak). A Chromolith RP-18e column (Merck, Kenilworth, NJ, 50 mm) was used for UPLC analysis, using an Agilent 1200 Liquid Chromatograph (Agilent, Omaha, NE). The products were analysed on a Bruker Impact II LC Q-TOF MS equipped with electrospray ionisation (ESI) in positive mode.

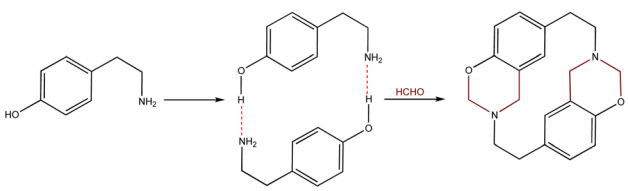

Scheme 1 4-Hydroxyphenylethylamine-related hydrogen bond-assisted macrocyclic synthesis.

Departamento de Química, Facultad de Ciencias, Universidad Nacional de Colombia, Sede Bogotá, Carrera 30 No. 45-03, Bogotá, Colombia. E-mail: arquevedop@unal.edu.co

† Electronic supplementary information (ESI) available. See DOI: https://doi.org/10.1039/d3ra08508b

Computational details

Computational calculations were carried out using the Gaussian 16 software package,[17–20] employing the non-local hybrid functional B3LYP with an empirical Grimme D3BJ dispersion term and the Pople's 6-31+G(d,p) basis set within the density functional theory (DFT) framework.[19–21] Interaction energies were corrected on the basis set superposition error (BSSE) to ensure accuracy by applying the counterpoise method.[22] This combination of functional and basis set has been proven to provide a proper geometrical and energy description including long-range dispersion contributions.[23]

Furthermore, the implicit and universal SMD solvation model was employed through single-point energy calculations to account for solvent effects on the geometries initially optimized in the gas phase.[24]

4-Hydroxybenzylamine 1 reaction with formaldehyde

Formaldehyde (37%, 5 mL) was added to a 4-hydroxybenzylamine **1** solution (500 mg, 4 mmol) in 10 mL solvent (ethanol, dioxane, DMF and acetonitrile). The mixture was kept without stirring at room temperature for 24 h; distilled water (15 mL) was then added, and product was extracted with dichloromethane (3 × 5 mL). The organic phase was washed with water (3 × 5 mL), dried with anhydrous sodium sulphate and concentrated. The resulting product was characterised by melting point, ultra-performance liquid chromatography-mass spectrometry (UPLC-MS) and nuclear magnetic resonance (NMR) spectroscopy (^{1}H and ^{13}C). The NMR spectra were obtained from the unpurified reaction products after removing the dichloromethane; the pure products were insoluble. In this article, the spectra of the product obtained from dioxane are analysed. The mass spectrum analysed corresponds to the pure product obtained from dioxane. The yields and melting points reported are those obtained from the pure products.

Azacyclophane 2

(1^3,1^4,3^3,3^4-tetrahydro-1^2H,3^2H–1,3(3,6)-bis(1,3-benzoxazine) cyclobutaphane):[27] $C_{18}H_{18}N_2O_2$. Yellow Solid, m.p. 190–192 °C. ^{1}H-NMR ($CDCl_3$), δ/ppm: 7.27–6.67 (aromatic protons), 4.89–4.75 (benzoxazinic methylenes), 4.01–3.66 (benzylic methylenes). ^{13}C-NMR ($CDCl_3$), δ/ppm: 153.6, 130.5, 130.2, 128.6, 128.4, 120.0, 116.4, 81.9, 55.1, 49.8. ESI-MS (m/z): 271.4143 [M + H-24]$^+$ (Calc. 271.4146), 136.0756 [M + 2H-12]$^{2+}$ (Calc. 136.0762). Yield: in ethanol: 52% (m.p. 190–192 °C), in dioxane: 55% (m.p. 190–192 °C), in DMF: 61% (m.p. 190–192 °C), in acetonitrile: 59% (m.p. 190–192 °C).

Results and discussion

Computational analysis

The formation of azacyclophane **2** from 4-hydroxybenzylamine **1** requires the pre-organisation of molecules into cyclic arrangements that facilitate macrocyclisation. This pre-organisation is achieved through the creation of a template, which is formed by establishing hydrogen bonds between two molecules, as illustrated in Scheme 2. The examined

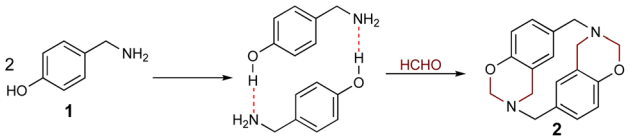

Scheme 2 4-hydroxybenzylamine **1** hydrogen bond-assisted macrocyclic synthesis.

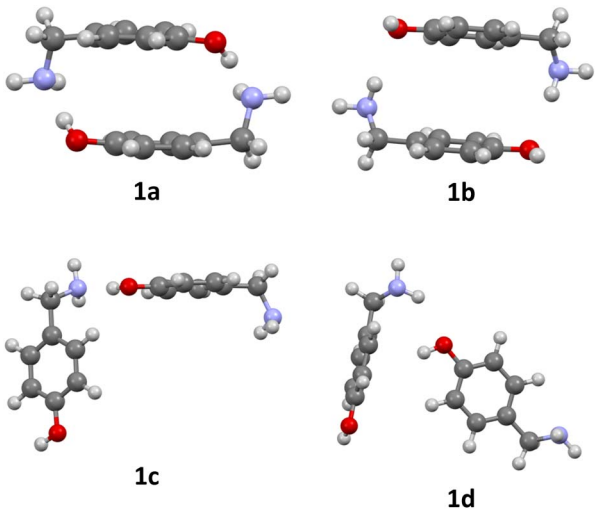

Fig. 1 Optimized dimers without dispersion terms of 1: O–H···N cyclic dimer (**1a**), N–H···O cyclic dimer (**1b**), O–H···N linear dimer (**1c**), N–H···O linear dimer (**1d**).

arrangements fall into two categories: linear and cyclic. These arrangements give rise to two distinct types of hydrogen bonds. The first type involves the hydroxyl group as the proton donor and the amino group as the acceptor (O–H···N), while the second type reverses these roles, with the amino group acting as the proton donor and the hydroxyl group as the acceptor (N–H···O), as depicted in Fig. 1.

To predict template formation, we calculated the enthalpy (ΔH^{gp}_{dim}) and the free energy of dimerization (ΔG^{gp}_{dim}) in gas phase. These parameters were determined through the following equations:

$$\Delta H^{gp}_{dim} = H^{gp}_{dimer} - 2H^{gp}_{4\text{–HOBA1}} \quad (1)$$

$$\Delta G^{gp}_{dim} = G^{gp}_{dimer} - 2G^{gp}_{4\text{–HOBA1}} \quad (2)$$

$$\Delta E^{gp}_{dim} = E^{gp}_{dimer} - 2E^{gp}_{4\text{–HOBA1}} \quad (3)$$

We incorporated a single point correction for dispersion interactions (GD3BJ) for the considered arrangements to account for long-range interactions.[21] These interactions are relevant in the case of cyclic dimers, where aromatic rings face each other, thereby engaging in π-stacking interactions.

According to the energy changes presented in Table 1, it can be noticed that the dimerization of **1** is only exergonic when dispersive interactions are considered. This indicates that dimerization occurs by hydrogen bonding and is further

Table 1 Thermodynamic parameters for the dimerization of compound **1** with single point (SP) dispersion correction

	B3LYP		
Struct.	ΔE_{dim}^{gp} (kcal mol^{-1})	ΔH_{dim}^{gp} (kcal mol^{-1})	ΔG_{dim}^{gp} (kcal mol^{-1})
1a	−18.6	−6.5	7.1
1b	−6.6	0.5	10.3
1c	−11.9	−6.8	2.2
1d	−7.1	−1.6	6.2
	SP B3LYP-D3BJ		
Struct.	ΔE_{dim}^{gp} (kcal mol^{-1})	ΔH_{dim}^{gp} (kcal mol^{-1})	ΔG_{dim}^{gp} (kcal mol^{-1})
1a	−18.6	−17.0	−3.8
1b	−6.6	−5.3	3.9
1c	−11.9	−10.1	−0.1
1d	−7.1	−5.7	3.1

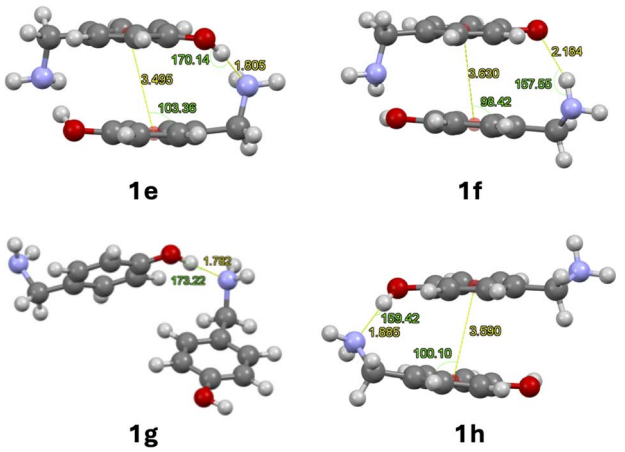

Fig. 2 Optimised dimers with dispersion terms of **1**: O–H···N cyclic dimer (**1e**), N–H···O cyclic dimer (**1f**), O–H···N linear dimer (**1g**), O–H···N linear dimer with stacking (**1h**).

stabilized by π-stacking. The linear and cyclic arrangements were optimised using dispersion terms to observe their influence on the geometry. The optimised structures are shown in Fig. 2.

No significant changes in geometry were observed for structures **1e–g** compared to structures **1a–c**. The linear arrangement with N–H···O hydrogen bond **1d** prefers to form a linear dimer with O–H···N hydrogen bond, stabilised by π stacking between its aromatic rings **1h**. Only the dimerization of **1e** and **1g** are exergonic according to Table 2.

The dispersion contribution, π-stacking energies and geometrical parameters for H-bond and π-stacking are detailed in Table 3. Centroid-plane angles were calculated between the plane of the aromatic ring and the centroid of the second aromatic ring using the software Mercury (Fig. 2).[25] The dispersion contribution of cyclic dimers was calculated using the following equations:[23]

$$\Delta E_D = \Delta E_{dim}^{gp,B3LYP\text{-}D} - \Delta E_{dim}^{gp,B3LYP} \quad (4)$$

Table 2 Thermodynamic parameters for the dimerization of compound **1** with dispersion correction

	B3LYP-D3BJ		
Struct.	ΔE_{dim}^{gp} (kcal mol^{-1})	ΔH_{dim}^{gp} (kcal mol^{-1})	ΔG_{dim}^{gp} (kcal mol^{-1})
1e	−19.8	−18.0	−3.5
1f	−8.9	−7.3	4.8
1g	−12.3	−10.5	−0.4
1h	−11.3	−9.6	2.0

$$\Delta H_D = \Delta H_{dim}^{gp,B3LYP\text{-}D} - \Delta H_{dim}^{gp,B3LYP} \quad (5)$$

$$\Delta G_D = \Delta G_{dim}^{gp,B3LYP\text{-}D} - \Delta G_{dim}^{gp,B3LYP} \quad (6)$$

In eqn (7), the π-stacking was estimated by considering the optimized geometry of all dimers and replacing the substituents on the aromatic ring with hydrogen atoms to obtain benzene rings. After that, single-point calculations were carried out on benzene dimers and monomers.

$$\Delta E_{\pi\text{-stacking}} = E_{\text{benzene dimer}}^{gp,D} - 2E_{benzene}^{gp,D} \quad (7)$$

Shorter H-bonds destabilize π-stacking due to steric repulsion, this effect is compensated by the increase in centroid-plane angles. The cyclic dimer **1e** is the most stable due to thermic effects and not due to geometric effects as shown in Table 3.

The significant enthalpic contribution from dispersive interactions, as shown in Table 3, decreases the substantial stabilization that **1g** experiences in contrast to **1e** due to π stacking between its aromatic rings and formation of two H-bonds. This fact makes the formation of **1e** more favoured thermodynamically.

In addition, to examine the relative populations of these two dimers, we have formulated the interconversion constant (K_{int}^{gp}). This constant is derived from the interplay between the dimerization constants of each process, as outlined in Scheme 3.

According to Scheme 3, the interconversion constant K_{int}^{gp} was computed at 298.15 K as follows:

$$K_{int}^{gp} = e^{\frac{\Delta G_{dim,linear}^{gp} - \Delta G_{dim,cyclic}^{gp}}{RT}} \quad (8)$$

This equation establishes a connection between the equilibrium concentrations of cyclic and linear dimers. For the dimers under consideration, K_{int}^{gp} was determined to be 1.81×10^2. This value strongly indicates a preference for cyclic dimers over linear ones. Hence, for **1**, the formation of cyclic arrangements featuring O–H···N hydrogen bonds, and further stabilized by π-stacking interactions between aromatic rings, is highly favoured.

Given the requirement of ethanol as a solvent for hydrogen bond-assisted macrocyclic synthesis, we explored various solvents to optimize the experimental conditions for the reaction of **1** (4-HOBA) with formaldehyde. To assess the

Table 3 Structural characterization and energy of dispersive interactions in dimers

				H-Bond		π−Stacking		
Struct	ΔE_D (kcal mol^{-1})	ΔH_D (kcal mol^{-1})	ΔG_D (kcal mol^{-1})	H-bond length O–H···N (Å)	H-bond angle O–H···N (°)	$\Delta E_{\pi\text{-stacking}}$ (kcal mol^{-1})	Centroid–centroid distance (Å)	Centroid-plane angle (°)
1e	−1.2	−11.5	−10.5	1.80	170.1	0.3	3.50	103.4
1f	−2.2	−7.8	−5.5	2.18	157.5	−1.3	3.63	98.4
1g	−0.4	−3.7	−2.6	1.78	173.2	—	—	—
1h	−4.3	−8.0	−4.2	1.88	159.4	−0.8	3.60	100.1

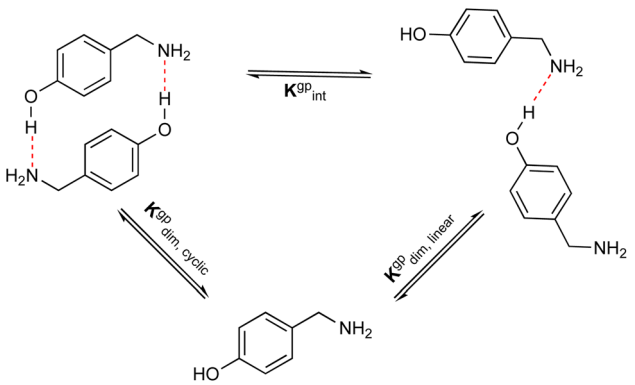

Scheme 3 Relationship between the dimerization and the interconversion constants.

thermodynamic feasibility in each solvent, we calculated ΔG^{sol}_{dim} using a thermodynamic cycle, as illustrated in Scheme 4.

The free energy changes in solution were calculated as follows:

$$\Delta G^{sol}_{dim} = \Delta G^{gp}_{dim} - 2\Delta G^{solv}_{4\text{-HOBA1}} + \Delta G^{solv}_{dimer} + \Delta G^{gp\rightarrow sol} \quad (9)$$

where ΔG^{gp}_{dim} is dimerization Gibbs energy change in gas phase, $\Delta G^{solv}_{4\text{-HOBA}}$ and ΔG^{solv}_{dimer} are Gibbs energy of solvation obtained with SMD solvation model. Since calculated gas phase free energies considered an ideal gas at 1 atm, a correction must be added to convert them to a standard state that uses a concentration in solution of 1 mol L^{-1}. This correction is as follows:[26]

$$\Delta G^{gp\rightarrow sol} = \Delta nRT \ln\left(\frac{1\ \text{mol/1 L}}{1\ \text{mol/24.46 L}}\right) = \Delta nRT \ln(24.46) \quad (10)$$

where Δn is the change in the number of species in reaction at 298.15 K.

The free energy changes in solution using different solvents are presented in Table 4. In this table the interconversion constants are also presented, to gain insight into the effect of each solvent in the preferences of linear or cyclic arrangements.

Notably, polar aprotic solvents such as dioxane, pyridine, and DMF emerge as strong proponents of cyclic dimer formation due to their limited interference with proton donor atoms. Toluene, a nonpolar solvent devoid of hydrogen bond interactions with the **1** molecule, also favours dimer formation.

In the context of hydrogen bond-assisted macrocyclic synthesis, an essential factor to consider is the solvent's compatibility with a 37% formaldehyde solution, as it affects solvents available for the reaction. While ethanol and

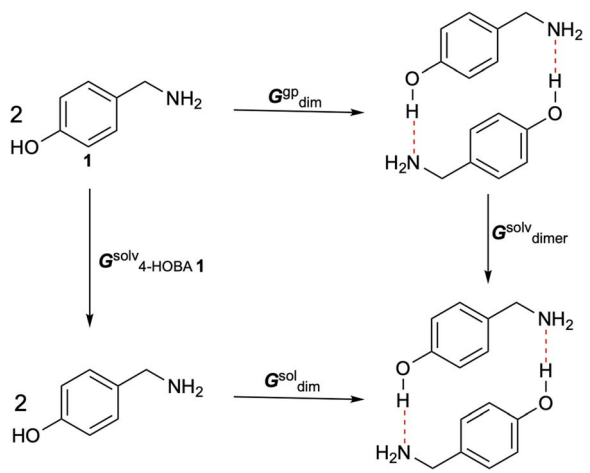

Scheme 4 Thermodynamic cycle for calculating the ΔG^{sol}_{dim} in the used solvents.

Table 4 Free energy changes in solution (kcal mol^{-1}) for the dimeric arrangements of **1**

Solvent	Dimeric structure	ΔG^{sol}_{dim} (kcal mol^{-1})	K^{sol}_{int}
Water	Cyclic	−2.0	2.4
	Linear	−1.5	
DMF	Cyclic	−4.1	19.0
	Linear	−2.4	
ACN	Cyclic	−2.9	6.0
	Linear	−1.8	
MeOH	Cyclic	−1.8	4.2
	Linear	−1.0	
EtOH	Cyclic	−1.7	3.4
	Linear	−0.1	
2-Propanol	Cyclic	−1.7	3.4
	Linear	−0.1	
Pyridine	Cyclic	−3.7	13.5
	Linear	−2.2	
DCM	Cyclic	−2.2	3.5
	Linear	−1.4	
Chloroform	Cyclic	−2.2	4.2
	Linear	−1.3	
Toluene	Cyclic	−3.9	24.0
	Linear	−2.0	
Dioxane	Cyclic	−5.0	88.0
	Linear	−2.4	

acetonitrile exhibit relatively lower K_{int}^{sol} values compared to other solvents, their ease of removal and low toxicity render them suitable choices for the reaction. Consequently, the solvents employed in the reaction included ethanol, DMF, acetonitrile, and dioxane.

4-Hydroxybenzylamine 1 reaction with formaldehyde

As stated above, it has been proposed that azacyclophane formation by hydrogen bond-assisted macrocyclic synthesis strategy depends on hydrogen bond template formation. Computational calculations have shown that 4-hydroxybenzylamine **1** in solution forms such templates; its reaction with formaldehyde will produce azacyclophane **2**, but only a mixture of linear oligomers **3** will be obtained if it forms linear arrangements (Scheme 5).

4-hydroxybenzylamine **1** reaction with formaldehyde was carried out using solvents selected by computational calculations. A solid **2** having a high melting point and low solubility was obtained with the four solvents used. Its ^{1}H-NMR spectra had broad signals, thereby hindering the determination of its multiplicity or integrals (Fig. 3); such pattern has been characteristic of previously synthesised 14-atom azacyclophanes.[11,12,28] It was observed in this spectrum that the substitution of the aromatic ring changed, and two new signals appeared in the aliphatic region, these signals were assigned to benzylic methylenes at 3.80 ppm and benzoxazinic methylenes at 4.83 ppm.

The signals expected for azacyclophane **2** appeared in ^{13}C-NMR spectrum (Fig. 3). Regarding characteristic signals, a signal was observed at 153.5 ppm indicating an aromatic carbon bound to –O–CH2–. Two signals should be observed in this region for linear product **3**, one for aromatic carbon bound to hydroxyl and another for aromatic carbon bound to –O–CH_2–. Three signals were observed in the aliphatic region; one at 81.9 ppm assigned to benzoxazinic methylenes and another two at 55.1 and 49.8 ppm assigned to benzylic methylenes (four signals should be observed for the linear product). Some low intensity signals were also observed, indicating a small percentage of linear products.

Azacyclophane **2** could not be differentiated from linear product **3** by heteronuclear multiple bond correlation (HMBC)

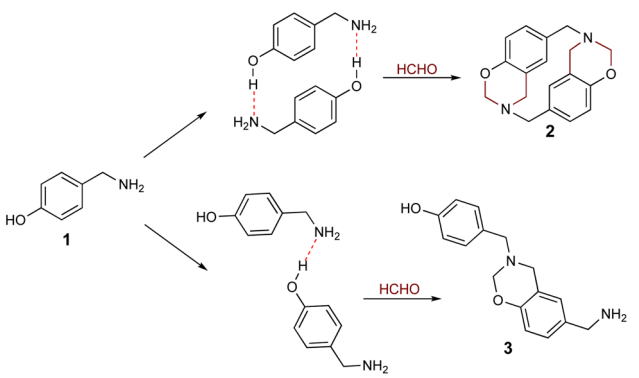

Scheme 5 Possible products from 4-hydroxybenzylamine **1** reaction with formaldehyde.

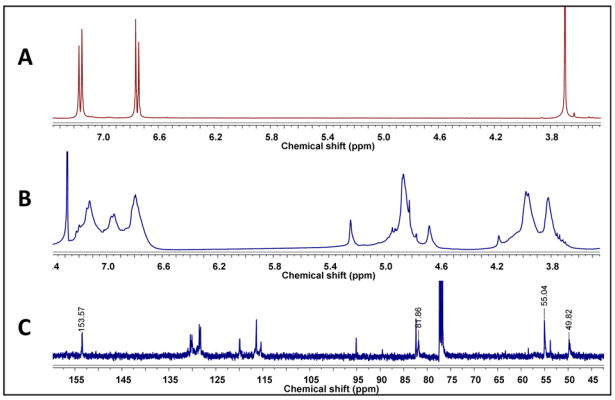

Fig. 3 (A) ^{1}H-NMR spectrum of **1**, (B) ^{1}H-NMR spectrum of azacyclophane **2**, (C) ^{13}C-NMR spectrum of azacyclophane **2**.

spectrum because they both had the same correlations. Key information was obtained when correlations between benzoxazinic hydrogens (at 4.84 ppm) with the carbon at 153.5 ppm and with the carbons assigned to the benzylic methylenes were observed (Fig. 4). It was also observed that signals at 4.2, 4.6 and 5.2 ppm in ^{1}H-NMR spectra did not correlate with any of the carbons assigned to azacyclophane **2**, thereby confirming that they were caused by formaldehyde polymerisation products.

The sample was dissolved in water : formic acid (0.1%) for UPLC-MS analysis due to poor azacyclophane **2** solubility; the product became partially dissolved in such conditions. Two peaks were observed in the chromatogram, having 0.5- and 0.7 min retention times. The first peak (0.5 min retention time) had two significant ions, the first at 271.1443 m/z $[M + H]^{+}$ and the second at 136.0756 m/z $[M + 2H]^{2+}$. These ions did not correspond to azacyclophane **2**, they represented azacyclophane **4**, which is a product of oxazine ring hydrolysis induced by adding formic acid (Scheme 6). Such hydrolysis is characteristic of the benzoxazines and occurs easily for benzoxazinic azacyclophanes.[29,30]

The second peak (0.7 min retention time) had three significant ions; the ion at 271.1440 m/z $[M + H]^{+}$ corresponding to linear dimer **3** (calc. 271.1441), this structure was confirmed by the ion at 259.1438 m/z $[M + H\text{-}12]^{+}$ (calc. 259.1441) and the ion at 242.1171 m/z $[M\text{-}28]^{+}$ (calc. 242.1176) (Fig. 5).

Mass spectra analysis enabled confirming that 4-hydroxybenzylamine **1** reaction with formaldehyde produced

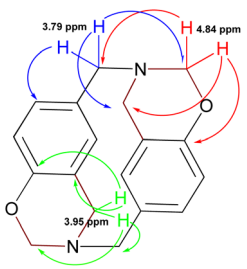

Fig. 4 Key correlations observed in azacyclophane **2** HMBC spectrum.

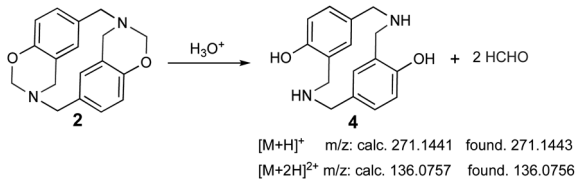

Scheme 6 Azacyclophane **2** hydrolysis and the main ions observed in (ESI)-MS spectrum.

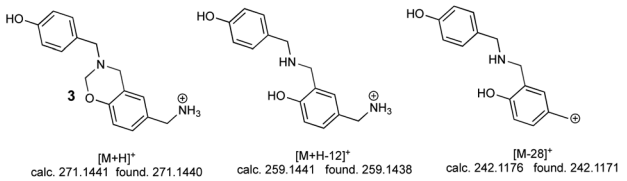

Fig. 5 The main ions observed in linear product **3** ESI-MS spectrum.

azacyclophane **2** as the major product, along with lower percentage yield of linear dimer **3**.

Conclusions

Computational calculations established that 4-hydroxybenzylamine can form dimers (templates) in gas phase and in solution by O–H···N hydrogen bonds; such cyclic dimers are stabilised by π-stacking. Cyclic dimer formation led to azacyclophane **2** being obtained *via* 4-hydroxybenzylamine **1** reaction with formaldehyde. The results demonstrated that hydrogen bond-assisted macrocyclic synthesis is a useful strategy for obtaining both 14- and 12-atom azacyclophane.

Author contributions

A. G-O. investigation, computational calculations, writing and original draft preparation. J. A-T. computational calculations supervisor, writing and original draft preparation. R. Q. conceptualization, supervision, writing and reviewing.

Conflicts of interest

There are no conflicts to declare.

Acknowledgements

We would like to thank the Universidad Nacional de Colombia for providing financial support (Research Project no. 57632).

Notes and references

1 H. Hopf and R. Gleiter, *Modern Cyclophane Chemistry*, Wiley-VCH: Federal Republic of Germany, 2004.
2 M. J. Van Eis, F. M. Bickelhaupt, S. Van Loon, M. Lutz, A. L. Spek, W. H. De Wolf, W. J. Van Zeist and F. Bickelhaupt, *Tetrahedron*, 2008, **64**, 11641.
3 A. V. Borounov, N. G. Lukyanenko, V. N. Pastushok, K. E. Krakowiak, J. S. Bradshaw, N. K. Dalley and X. Kou, *J. Org. Chem.*, 1995, **60**, 4912.
4 P. Rajakumar and A. M. A. Rasheed, *Tetrahedron*, 2005, **61**, 5351.
5 E. García-Espaňta and S. V. Luis, *Supramol. Chem.*, 1996, **6**, 257.
6 E. García-España, P. Díaz, J. M. Llinares and A. Bianchi, *Coord. Chem. Rev.*, 2006, **250**, 2952.
7 M. Arunachalam, I. Ravicumar and P. Ghosh, *J. Org. Chem.*, 2008, **73**, 9144.
8 M. Sato, F. Uehara, K. Sato, M. Yamaguchi and C. Kabuto, *J. Am. Chem. Soc.*, 1999, **121**, 8270.
9 H. Stetter and E. Roos, *Chem. Ber.*, 1955, **88**, 1390.
10 G. Faust and M. Pallas, *J. Prakt. Chem.*, 1960, **11**, 146.
11 N. Nuñez-Dallos, A. Reyes and R. Quevedo, *Tetrahedron Lett.*, 2012, **53**, 530.
12 R. Quevedo and B. Moreno-Murillo, *Tetrahedron Lett.*, 2009, **50**, 936.
13 C. Díaz-Oviedo and R. Quevedo, *J. Mol. Struct.*, 2020, **1202**, 127283.
14 C. Díaz-Oviedo and R. Quevedo, *Rev. Colomb. Quim.*, 2018, **47**, 5.
15 N. Nuñez-Dallos, C. Díaz-Oviedo and R. Quevedo, *Tetrahedron Lett.*, 2014, **55**, 4216.
16 S. Chaves, M. Macías and R. Quevedo, *J. Mol. Struct.*, 2023, **1298**, 137079.
17 M. J. Frisch, G. W. Trucks, H. B. Schlegel, G. E. Scuseria, M. A. Robb, J. R. Cheeseman, G. Scalmani, V. Barone, G. A. Petersson, H. Nakatsuji, X. Li, M. Caricato, A. V. Marenich, J. Bloino, B. G. Janesko, R. Gomperts, B. Mennucci, H. P. Hratchian, J. V. Ortiz, A. F. Izmaylov, J. L. Sonnenberg, D. Williams-Young, F. Ding, F. Lipparini, F. Egidi, J. Goings, B. Peng, A. Petrone, T. Henderson, D. Ranasinghe, V. G. Zakrzewski, J. Gao, N. Rega, G. Zheng, W. Liang, M. Hada, M. Ehara, K. Toyota, R. Fukuda, J. Hasegawa, M. Ishida, T. Nakajima, Y. Honda, O. Kitao, H. Nakai, T. Vreven, K. Throssell, J. A. Montgomery, Jr., J. E. Peralta, F. Ogliaro, M. J. Bearpark, J. J. Heyd, E. N. Brothers, K. N. Kudin, V. N. Staroverov, T. A. Keith, R. Kobayashi, J. Normand, K. Raghavachari, A. P. Rendell, J. C. Burant, S. S. Iyengar, J. Tomasi, M. Cossi, J. M. Millam, M. Klene, C. Adamo, R. Cammi, J. W. Ochterski, R. L. Martin, K. Morokuma, O. Farkas, J. B. Foresman and D. J. Fox, *Gaussian 16, Revision C.01*, Gaussian, Inc., Wallingford CT, 2016.
18 A. R. Allouche, *J. Comput. Chem.*, 2011, **32**, 174.
19 A. D. Becke, *J. Chem. Phys.*, 1993, **98**, 5648.
20 C. Lee, W. Yang and R. G. Parr, *Phys. Rev. B*, 1988, **37**, 785.
21 S. Grimme, S. Ehrlich and L. Goerigk, *J. Comput. Chem.*, 2011, **32**, 1456.
22 S. F. Boys and F. Bernardi, *Mol. Phys.*, 1970, **19**, 553.
23 J. Alí-Torres, A. Rimola, C. Rodríguez-Rodríguez, L. Rodríguez-Santiago and M. Sodupe, *J. Phys. Chem. B*, 2013, **117**, 6674.
24 A. V. Marenich, C. J. Cramer and D. G. Truhlar, *J. Phys. Chem. B*, 2009, **113**, 6378.

25 C. F. Macrae, I. Sovago, S. J. Cottrell, P. T. A. Galek, P. McCabe, E. Pidcock, M. Platings, G. P. Shields, J. S. Stevens, M. Towler and P. A. Wood, *J. Appl. Crystallogr.*, 2020, **32**, 226–235.
26 J. Alí-Torres, L. Rodríguez-Santiago and M. Sodupe, *Phys. Chem. Chem. Phys.*, 2011, **13**(17), 7852.
27 K. Hirayama, *Tetrahedron Lett.*, 1972, **13**, 2109.
28 R. Quevedo, *J. Mol. Struct.*, 2020, **1207**, 127777.
29 R. Quevedo, M. González and C. Díaz-Oviedo, *Tetrahedron Lett.*, 2012, **53**, 1595.
30 R. Quevedo, I. Ortiz and A. Reyes, *Tetrahedron Lett.*, 2010, **51**, 1216.